Hindawi
Journal of Sensors
Volume 2024, Article ID 9807937, 1 page
https://doi.org/10.1155/2024/9807937

Retraction

Retracted: Research on Path Planning Method of Unmanned Boat Based on Improved DWA Algorithm

Journal of Sensors

Received 23 January 2024; Accepted 23 January 2024; Published 24 January 2024

This article has been retracted by Hindawi following an investigation undertaken by the publisher [1]. This investigation has uncovered evidence of one or more of the following indicators of systematic manipulation of the publication process:

(1) Discrepancies in scope
(2) Discrepancies in the description of the research reported
(3) Discrepancies between the availability of data and the research described
(4) Inappropriate citations
(5) Incoherent, meaningless and/or irrelevant content included in the article
(6) Manipulated or compromised peer review

The presence of these indicators undermines our confidence in the integrity of the article's content and we cannot, therefore, vouch for its reliability. Please note that this notice is intended solely to alert readers that the content of this article is unreliable. We have not investigated whether authors were aware of or involved in the systematic manipulation of the publication process.

Wiley and Hindawi regrets that the usual quality checks did not identify these issues before publication and have since put additional measures in place to safeguard research integrity.

We wish to credit our own Research Integrity and Research Publishing teams and anonymous and named external researchers and research integrity experts for contributing to this investigation.

The corresponding author, as the representative of all authors, has been given the opportunity to register their agreement or disagreement to this retraction. We have kept a record of any response received.

References

[1] L. Zhang, Y. Han, and B. Jiang, "Research on Path Planning Method of Unmanned Boat Based on Improved DWA Algorithm," *Journal of Sensors*, vol. 2022, Article ID 9315483, 10 pages, 2022.

Hindawi
Journal of Sensors
Volume 2022, Article ID 9315483, 10 pages
https://doi.org/10.1155/2022/9315483

Research Article

Research on Path Planning Method of Unmanned Boat Based on Improved DWA Algorithm

Lanyong Zhang,[1] **Yu Han**,[1] **and Bo Jiang**[2]

[1]*College of Intelligent Science and Engineering, Harbin Engineering University, Harbin 150000, China*
[2]*The 27th Research Institute of China Electronics Technology Group Corporation, Zhengzhou 450047, China*

Correspondence should be addressed to Lanyong Zhang; zhanglanyong@hrbeu.edu.cn

Received 14 July 2022; Accepted 24 August 2022; Published 23 September 2022

Academic Editor: Yuan Li

Aiming at the problem of local path planning for unmanned surface vehicles, the traditional dynamic window algorithm (DWA) has the problems of uneven obstacle avoidance path and poor adaptability to complex environments. This paper proposes a local path planning method based on improved DWA. The evaluation item that replaces the direction angle difference with the target distance is used to avoid the path from being unsmooth due to vibration. And the fuzzy logic control algorithm is introduced to dynamically adjust the weight value of the trajectory evaluation function to complete the path optimization. The introduction of the A∗ algorithm is designed to preplan the map environment and extract key turning points as subtarget points of the local obstacle avoidance algorithm to enhance the path optimization ability. The simulation results show that the improved DWA algorithm can shorten the planned path length by 23.4% and the path smoothness by 34.8%, enabling USV to find a reasonable, efficient, and smooth path in complex environments.

1. Introduction

The unmanned surface vehicle (USV) [1] has the characteristics of fast speed and strong maneuverability and modularity and is the most typical unmanned system equipment. The mission of the USV system cluster in the combat field has expanded from intelligence reconnaissance and surveillance to mine warfare, antisubmarine warfare, and special operations support [2, 3].

The existing unmanned surface boats have a single type and model and have simple tasks and functions, so they cannot undertake naval combat tasks in the new era, especially that their autonomous navigation capabilities are weak [4]. In the strong dynamic and unstructured marine environment, in order to achieve the navigation requirements of intelligent autonomous level, USV needs perfect and efficient control technologies such as path planning, autonomous navigation, and obstacle avoidance to ensure safety [5].

Path planning is aimed at finding an efficient and safe navigation route from the starting position to the target area, which can be divided into global path planning and local path planning [6]. Global path planning is to use prior information to calculate the optimal route from the starting point to the target point offline. Local path planning detects and processes unknown obstacles on the preplanned path and autonomously avoids obstacles, so as to plan a feasible route online. Unknown obstacles or other interference factors are prone to appear in the nonstructural environment at sea. In order to ensure real-time security and reliability, it is necessary to combine the characteristics of the two to build a multilayer obstacle avoidance structure. The proposed USV obstacle avoidance algorithms can all ensure the basic driving safety of USVs. The difference lies in the obstacle avoidance accuracy, computational complexity, and applicable scenarios of different algorithms [7]. The artificial potential field method and the DWA algorithm can be combined to use the collision risk index and relative distance to evaluate the danger of moving obstacles [8], so as to quickly react and avoid moving obstacles.

Taking into account the constraints of USV's own kinematics, safety, smoothness, and planning time, the

improvement of local path planning performance can effectively improve the operating efficiency of USV in complex water environment, reduce energy consumption, and save costs.

Yan et al. [9] proposed the generalized speed obstacle method in view of the limitation of the original speed obstacle method based on strong assumptions. Simulation shows that the generalized speed obstacle method is more suitable for collision avoidance of close-range ships. Seder and Petrovic [10] improved on the DWA proposed by Fox, using moving grid to model dynamic obstacles, by predicting the collision point position between USV and dynamic obstacles and constructing a virtual obstacle at this position, from the feasible speed. Select the appropriate speed control command in the space to achieve local obstacle avoidance.

Chang et al. [11] used the reinforcement learning method to adjust the DWA parameters to complete the improvement and expansion of the evaluation function, which improved the planning efficiency, but the real-time performance was poor. Liu et al. [12] integrated the improved A∗ with the DWA algorithm, but the improved A∗ algorithm has insufficient adaptability and is difficult to deal with complex dynamic environments. Xu et al. [13] used particle swarm optimization to optimize the parameters of artificial potential field method and combined with fuzzy rules to avoid obstacles, but their fuzzy rules tended to stay away from moving obstacles and could not flexibly deal with moving obstacles. Bai et al. [14] proposed a path planning algorithm based on A∗ and DWA. The key points of the global path were selected as the subtarget points of the local path planning, and the global optimal path evaluation subfunction was constructed. The evaluation function is adaptively adjusted according to obstacle and environmental information to optimize the performance of the DWA algorithm in local optimization and planning time. Under the premise of the optimal path, the efficiency and safety of the real-time path of the unmanned system are effectively improved.

In this paper, by introducing the derivative of the target distance to replace the direction angle evaluation item, the smoothness and path length of the obstacle avoidance path are optimized, and the fuzzy logic controller is integrated at the same time, and the information obtained by the obstacle detection model is used as the input of the fuzzy controller to evaluate the weight of the item. As the output of the controller, dynamically adjust the weight according to the distribution of obstacles, so as to enhance the adaptability of the DWA algorithm to the complex environment.

2. USV Model

2.1. USV Kinematic Model. Since the USV moves at sea level and the movement in the vertical direction is small, this paper ignores the movement of the USV in the vertical direction, simplifies the movement space of the USV into a two-dimensional plane, and establishes the USV kinematic model

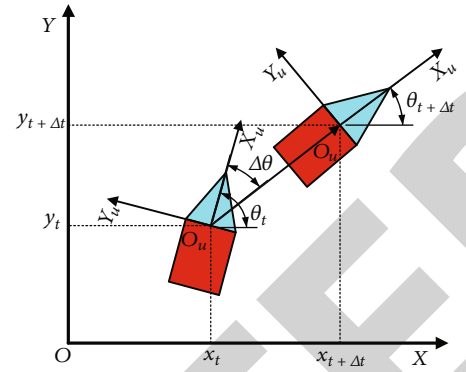

Figure 1: USV kinematic model.

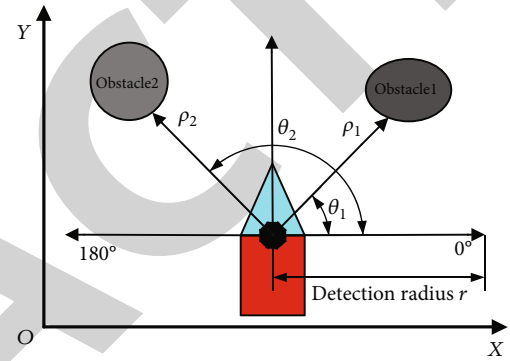

Figure 2: Obstacle detection model.

as shown in Figure 1, but simplifying the model weakens the accuracy of the model and the effectiveness of the control.

XOY represents the map coordinate system, $X_uO_uY_u$ represents the USV coordinate system, and θ_t and $\theta_{t+\Delta t}$ represent the attitude angle of the USV at time t and time $t + \Delta t$ (the angle between the X_u of the USV coordinate system and the x-axis of the map coordinate system).

2.2. Obstacle Detection Model. In this paper, an obstacle detection model is established to obtain the distance information between the USV and the obstacle and the orientation information of the obstacle relative to the USV.

The detection radius is set as r, and the range within the detection radius r is scanned and detected in unit time. When the obstacle is outside the detection radius r, the distance between the USV and the obstacle is set to be infinite. The i-th detection information is set to include the distance ρ_i between the USV and the obstacle and the azimuth θ_i of the obstacle relative to the USV, as shown in Figure 2.

2.3. Principle of DWA. DWA is proposed on the basis of the curvature velocity method, which transforms the position control of the USV into the velocity control according to the corresponding relationship between the position and the velocity of the USV. The core idea of DWA is to form an achievable velocity space of linear velocity v and angular velocity w according to the constraints of the USV's own motion characteristics and the safety distance of obstacles.

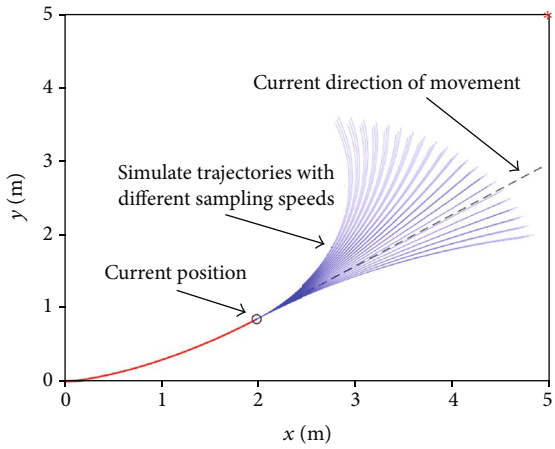

Figure 3: Simulated trace of sampling speed.

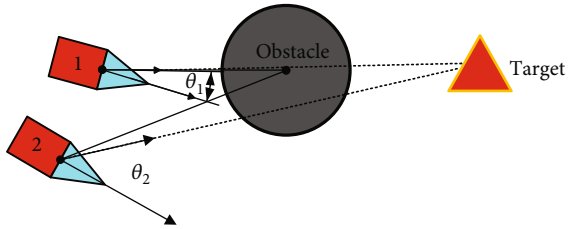

Figure 4: Schematic diagram of obstacle avoidance model.

The velocity space is sampled in unit time, and multiple sets of linear and angular velocities (v, w) are sampled, hereinafter referred to as velocity, and the motion trajectory of each set of velocities in a certain period of time is simulated according to the USV kinematic model. A set of velocities uniquely determines an arc trajectory, and the arc trajectory radius R_i and velocity satisfy

$$R_i = \frac{v_i}{w_i}. \tag{1}$$

In (3), when $w_i \neq 0$ and $R_i < \infty$, it is an arc trajectory; when $w_i = 0$ and $R_i = \infty$, it is a straight trajectory at this time. The optimal speed control command in the speed space is obtained through the trajectory evaluation function to control the speed of the USV at each moment.

2.3.1. Speed Space. The speed space consists of multiple groups of achievable speeds (v, w), and the speed command of the USV is generated from the search in the speed space. The velocity space is constrained by the USV's own kinematic characteristics, maximum and minimum velocity constraints, and safety constraints.

The USV velocity constraint includes the linear velocity size v and the angular velocity size w, and the maximum and minimum velocity space is represented as v_m.

$$v_m = \{v \in [0, v_{\max}], w \in [-w_{\max}, w_{\max}]\}. \tag{2}$$

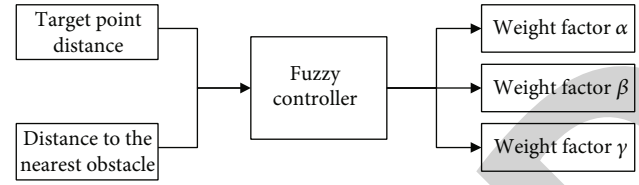

Figure 5: Fuzzy logic controller block diagram.

In (4), $v_{\max}$ and $w_{\max}$ represent the maximum linear velocity and maximum angular velocity that the USV can achieve, respectively.

Considering that the USV's own mobility is limited by the driving force, there are upper limits on linear acceleration and angular acceleration. Given the current linear velocity v_c, the current angular velocity w_c, and the time interval Δt, the velocity space that the USV can reach at the next moment is expressed as v_d.

$$v_d = \left\{ (v, w) \middle| \begin{matrix} v \in [v_c - a_m \Delta t, v_c + a_m \Delta t] \\ w \in [w_c - \alpha_m \Delta t, w_c + \alpha_m \Delta t] \end{matrix} \right\}. \tag{3}$$

In (3), a_m and α_m represent the maximum linear acceleration and the maximum angular acceleration of the USV, respectively.

In order to ensure that the USV can stop before encountering an obstacle, from the perspective of safety, under the condition of maximum acceleration, the allowable speed without collision is v_a.

$$v_a = \left\{ (v, w) \middle| \begin{matrix} v \leq \sqrt{2 \cdot \mathrm{dist}(v, w) \cdot a_m} \\ w \leq \sqrt{2 \cdot \mathrm{dist}(v, w) \cdot \alpha_m} \end{matrix} \right\}. \tag{4}$$

In (4), $\mathrm{dist}(v, w)$ represents the closest distance between the end position of the trajectory simulated by the current speed and the obstacle.

Taking the above considerations into account, the intersection formed by the above three velocity constraints is used as the final velocity space, and the velocity space is represented by $\mathbf{v_s}$, as shown in

$$v_s = v_m \cap v_d \cap v_a. \tag{5}$$

After discretizing the velocity space, multiple sets of samples are performed. Set the velocity sampling resolution to 0.01 m/s, the angular velocity sampling resolution to 1 deg/s, and the simulation time to 5 seconds. The simulated trajectory at the corresponding sampling speed is shown in Figure 3.

It can be seen that the trajectory simulated by the constrained velocity space presents arc and straight lines. The trajectory of each speed simulation is evaluated by the trajectory evaluation function, and the most suitable trajectory corresponding to the speed command is selected as the speed control command of the USV at the next moment.

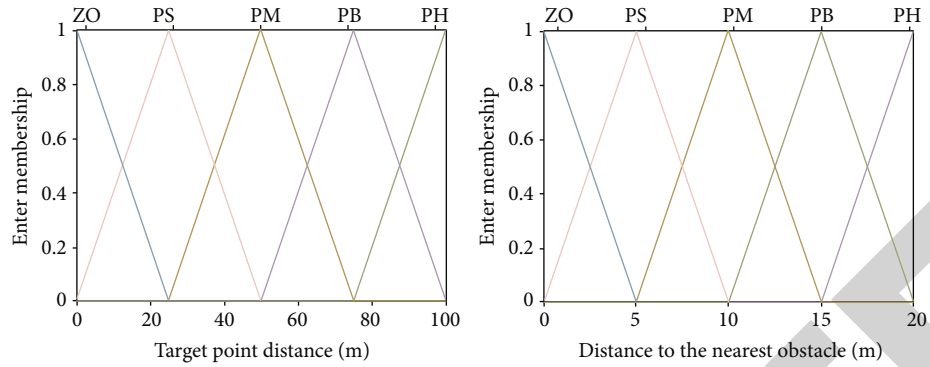

Figure 6: Membership function of input.

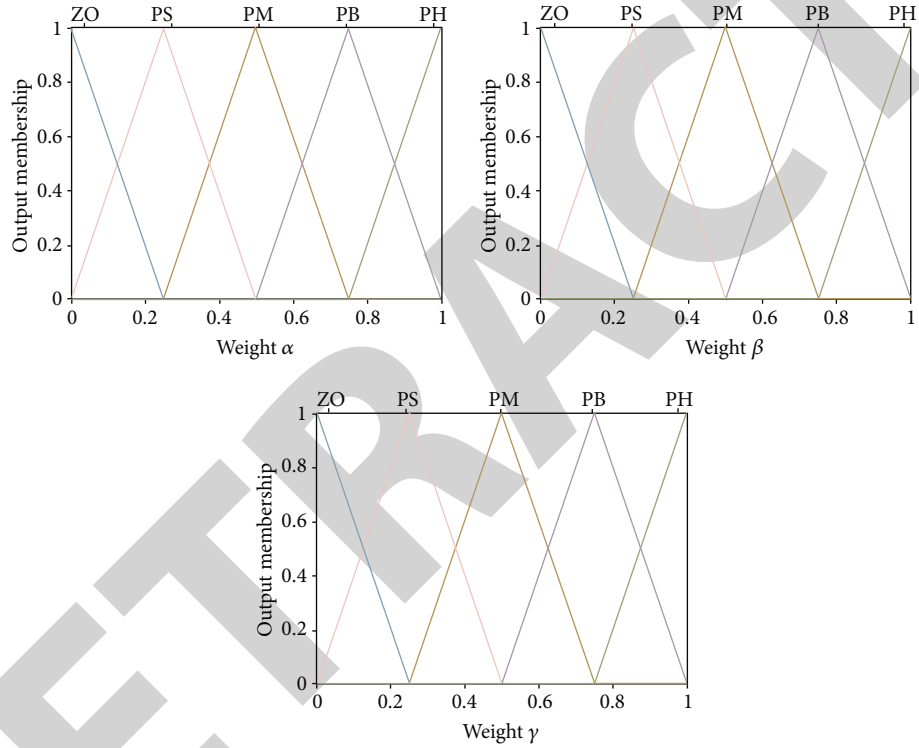

Figure 7: Membership function of output.

Table 1: Fuzzy rule for weight α.

Distance	Obstacle distance				
	ZO	PS	PM	PB	PH
ZO	PM	PB	PB	PH	pH
PS	PS	PM	PB	PB	PH
PM	ZO	PS	PM	PB	PB
PB	ZO	ZO	PS	PM	PB
PH	ZO	ZO	ZO	PS	PM

2.3.2. Trajectory Evaluation Function. The design criterion of the evaluation function is to make the USV avoid obstacles as much as possible and move towards the target point quickly in the process of local obstacle avoidance. The designed evaluation function is

$$G(v, w) = \alpha \cdot \text{head}(v, w) + \beta \cdot \text{dist}(v, w) + \gamma \cdot \text{vel}(v, w), \quad (6)$$

$$\alpha + \beta + \gamma = 1, \quad (7)$$

$$v_{\text{cmd}} = \{(v, w) \in \max G(v, w)\}. \quad (8)$$

In (6), $\text{head}(v, w)$ is the directional angle evaluation function, which represents the directional angle deviation between the direction of the end point of the simulated trajectory and the target at the current speed; $\text{dist}(v, w)$ is the distance evaluation function, which represents the closest distance to the obstacle on the trajectory corresponding to the speed; $\text{vel}(v, w)$ is the evaluation function of the current speed magnitude. In (7), α, β, and γ are the weights of the three evaluation functions. (8) indicates that the speed corresponding to the maximum value of the evaluation function (v, w) is the speed command at the next moment.

Table 2: Fuzzy rule for weight β.

Distance	Obstacle distance				
	ZO	PS	PM	PB	PH
ZO	PS	PS	ZO	ZO	ZO
PS	PM	PS	PS	ZO	ZO
PM	PB	PM	PS	PS	ZO
PB	PH	PB	PM	PS	PS
PH	PH	PH	PB	PM	PS

Table 3: Fuzzy rule for weight γ.

Distance	Obstacle distance				
	ZO	PS	PM	PB	PH
ZO	ZO	ZO	ZO	ZO	PS
PS	ZO	ZO	ZO	PS	PM
PM	ZO	ZO	PS	PM	PB
PB	ZO	PS	PM	PB	PH
PH	PS	PS	PM	PB	PH

3. Improved DWA and Its Application

3.1. Optimize Evaluation Items. When the USV approaches the target point, if there is an obstacle blocking the direction of the USV, the USV will naturally perform the obstacle avoidance operation, but during the obstacle avoidance process, changes in the heading angle of the USV cause different responses. When the value increases, the speed command selection at this time is different on whether to avoid obstacles to increase the distance from the obstacle or to reduce the difference in the direction angle, which leads to the oscillation of the obstacle avoidance path. The obstacle avoidance model is shown in Figure 4.

In addition, as the USV approaches the target point, the angle θ between the USV's heading and the target gradually increases. Under the action of the azimuth evaluation function $\text{head}(v, w)$, the UAV will increase its own angular velocity w to reduce the included angle θ, resulting in the movement of the USV to be uncontrollable.

In view of the defect that the obstacle avoidance path of DWA is not smooth, the original direction angle evaluation item is replaced, and the derivative of the target distance is introduced to replace the azimuth angle. The improved trajectory evaluation function is as follows:

$$G(v, w) = \alpha \cdot \text{gdist}(v, w) + \beta \cdot \text{odist}(v, w) + \gamma \cdot \text{vel}(v, w), \tag{9}$$

$$\text{gdist}(v, w) = \rho_{\text{goal}} = \frac{1}{2\sqrt{(x_c - x_g)^2 + \left(y_c - y_g\right)^2}}. \tag{10}$$

In (9), $\text{gdist}(v, w)$ represents the derivative of the distance between the end of the simulated trajectory corresponding to the speed (v, w) and the target point, and $\text{odist}(v, w)$ represents the distance between the end of the simulated trajectory corresponding to the speed (v, w) and the nearest obstacle. In (10), (x_c, y_c) and (x_g, y_g) represent the current position coordinates and target point coordinates of the USV, respectively. It can be seen from (10) that the derivative value of the target distance increases with the decrease of the distance between the USV and the target point. When the USV is closer to the target point, its proportion begins to increase, and the optimization goal of the evaluation function is to approach the target point and avoid obstacles. Therefore, the defect that the path is not smooth during the obstacle avoidance process is solved.

3.2. Fusion Fuzzy Control Algorithm. The selection of DWA's speed control command has a great relationship with the weight of each part of the evaluation function, and the obstacle avoidance path should be optimized as much as possible under the condition of ensuring the success of obstacle avoidance. The path found by a single weight is not ideal, and the weight of the trajectory evaluation function needs to be adjusted in real time.

The fuzzy logic control system is a rule-based control algorithm, which does not require an accurate mathematical model of the USV that is difficult to model, and can simulate human thinking only based on language control. The fuzzy logic controller consists of five main parts, namely, defining variables, fuzzification, knowledge base, logical judgment, and defuzzification.

According to the above content, a fuzzy controller with two inputs and three outputs is designed. First, the input variables of the fuzzy logic controller are determined as the distance between the USV and the target point and the distance between the USV and the nearest obstacle, and the outputs are, respectively, in the trajectory evaluation function of the DWA algorithm. The weights of each evaluation item are α, β, and γ, as shown in Figure 5.

The input and output variables of the fuzzy logic controller use a continuous domain of universe. The fuzzy logic controller is designed to adjust the weight coefficient of the trajectory evaluation function of the USV when avoiding obstacles. Therefore, the distance between the USV and the target point is set as $[0, 100]$, and the fuzzy set is {ZO , PS, PM, PB, PH}, when the distance between the USV and the target point is greater than 100 m, let it be equal to 100. Since the safe distance between the USV and the obstacle is 20 m, the universe of discourse for the distance between the USV and the nearest obstacle is set to $[0, 20]$, and the fuzzy set is {ZO, PS, PM, PB, PH}. When the distance of the nearest obstacle is greater than 20 m, set it equal to 20. The domain of discourse of the weight coefficients α, β, and γ of the evaluation function are all $[0, 1]$, and the corresponding fuzzy subsets are all {ZO, PS, PM, PB, PH}. The corresponding meanings of the above fuzzy sets are{ZO, PS, PM, PB, PH}.

Due to the simple and rapid operation of the triangular distributed fuzzy variables, the triangular function is used as the membership function for the input and output variables. The membership function curve of the input variable is shown in Figure 6, and the membership curve of the output variable is shown in Figure 7.

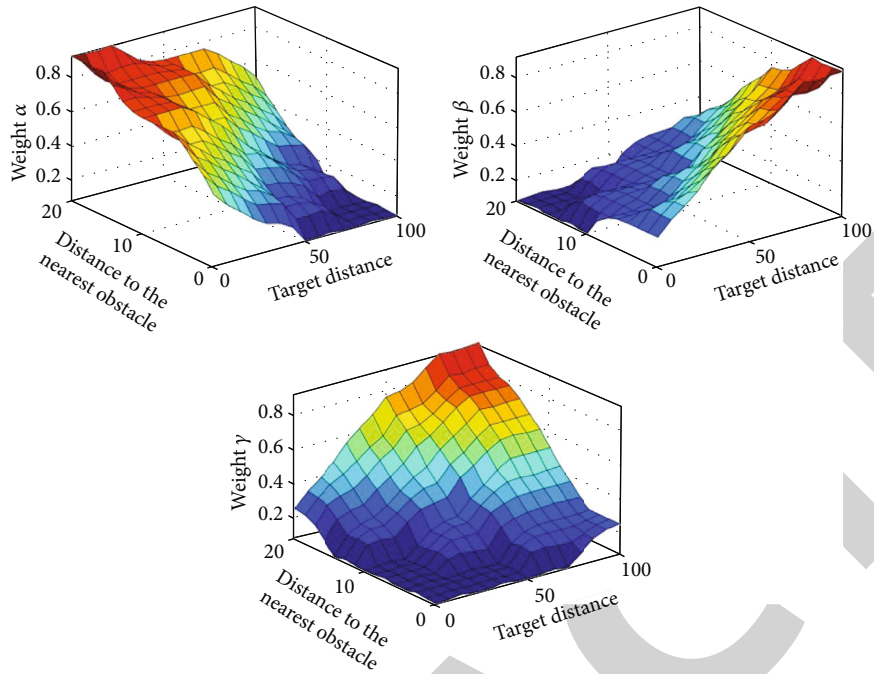

Figure 8: Correspondence between input value and output value.

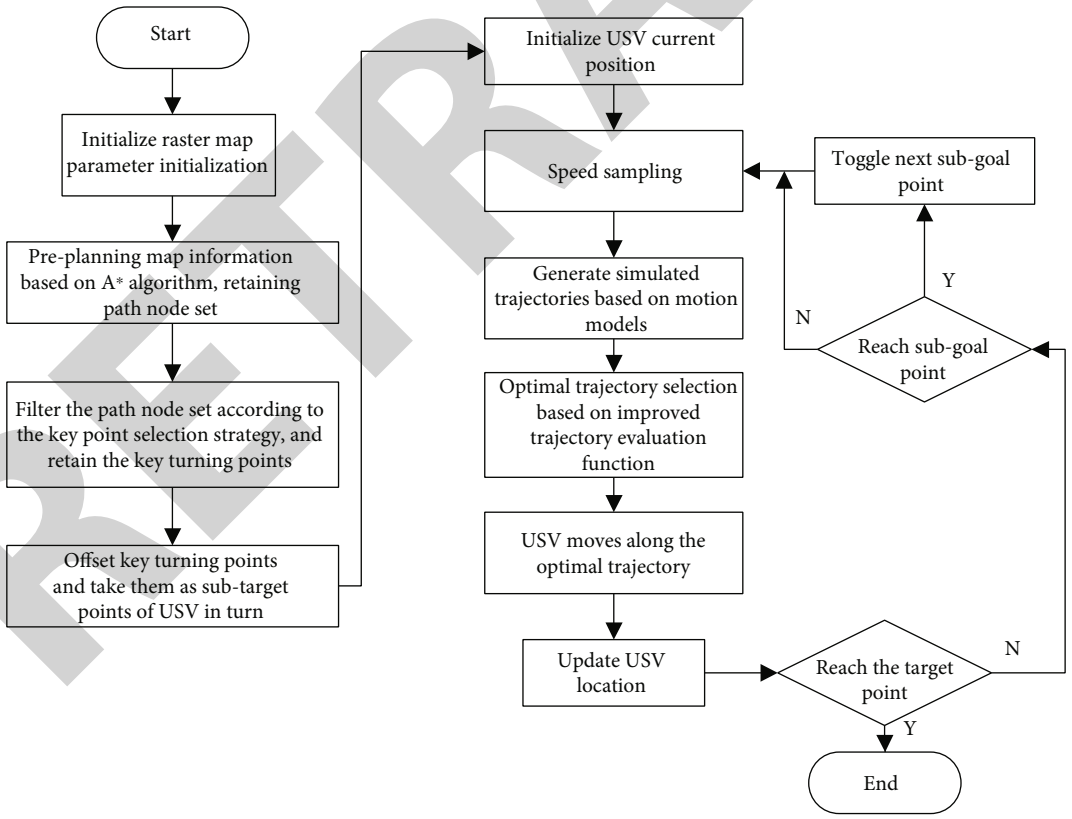

Figure 9: Flow chart of fusion A∗ and DWA algorithm.

According to the fuzzy subsets of the fuzzy variables defined above, the fuzzy control rules can be summarized as follows.

Rule 1: when the distance between the USV and the target point and the distance between the USV and the nearest obstacle are large, the USV does not need to rush to avoid

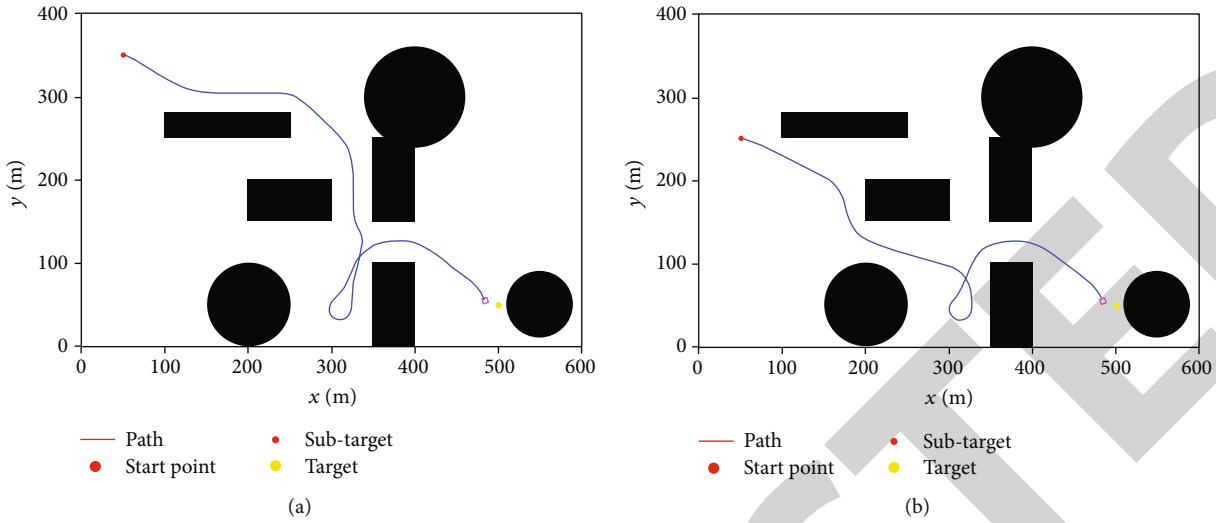

Figure 10: Original DWA path planning simulation results.

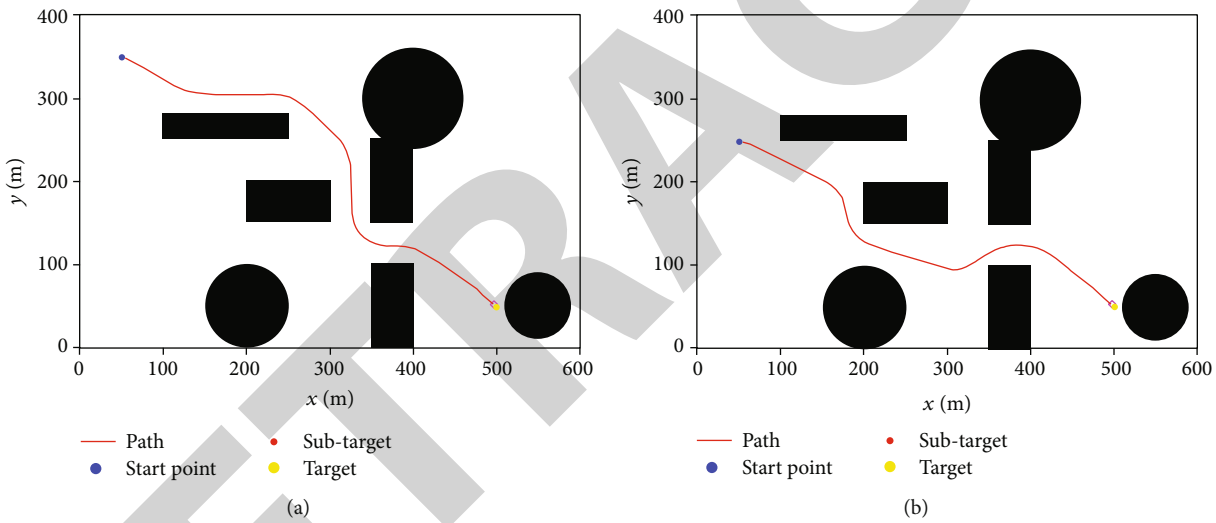

Figure 11: Improved DWA path planning simulation results.

obstacles at this time. At this time, the selected value of γ is large, the value of α is moderate, and the value of β is small

Rule 2: when the distance between the USV and the target point is large and the distance from the nearest obstacle is small, the USV should give priority to avoiding obstacles at this time, not in a hurry to approach the target point, and reduce the forward speed. At this time, the selected β value is larger, and the α and γ values are smaller

Rule 3: when the distance between the USV and the target point is small and the distance from the nearest obstacle is large, the USV should first approach the target point, not in a hurry to avoid obstacles, and reduce the forward speed. At this time, the selected value of α is larger, and the values of β and γ are smaller

Rule 4: when the distance between the USV and the target point and the distance to the nearest obstacle are both small, the USV should first approach the target point, avoid obstacles moderately, and reduce the forward speed. At this time, the selected value of α is large, the value of β is moderate, and the value of γ is small

To sum up, the fuzzy rule table for establishing the weight (α, β, γ) of each evaluation item of the DWA trajectory evaluation function is shown in Tables 1, 2 and 3.

According to the fuzzy rule table established above, the relationship between input and output can be obtained. Mamdani-type reasoning is used for fuzzy decision-making. The relationship between the input and output of the fuzzy controller is shown in Figure 8.

It can be seen from Figure 8 that the sizes of α, β, and γ are jointly determined by the distance between the USV and the target point and the distance to the nearest obstacle, and their changing trends conform to the established fuzzy control rules.

Fuzzy logic control adopts the Mamdani method for reasoning, and the obtained values of α, β, and γ are fuzzy quantities. In this paper, the centroid method is used to

Table 4: Comparison of DWA algorithm path evaluation index results.

Algorithm simulation example	Path length (m)	Smoothness	Security	Time (s)
Traditional (a)	809.8	2.66	99	34.81
Traditional (b)	677.2	2.56	95	28.32
This paper (a)	604.1	1.68	113	37.32
This paper (b)	534.2	1.72	90	34.61

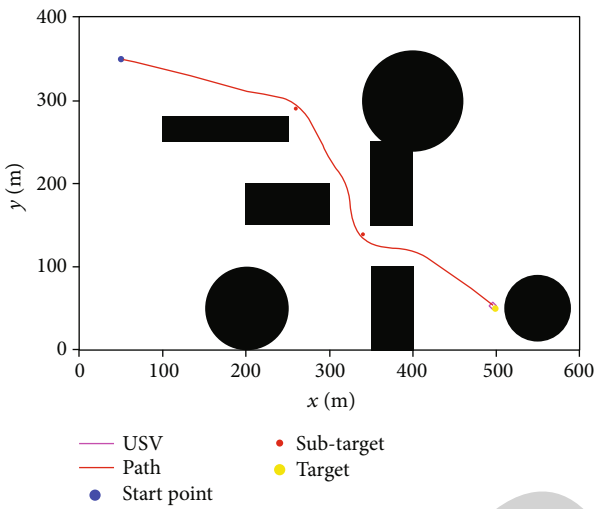

Figure 12: Fusion algorithm path planning simulation results.

defuzzy α, β, and γ to determine the specific weight values. By viewing the rule observer window, the specific output values of α, β, and γ can be obtained when a certain input value is determined and then normalized to give the weight of each evaluation item in the trajectory evaluation function.

3.3. Improved DWA with A∗ Algorithm. The key turning points in the path node set planned by the A∗ algorithm are extracted as the subtarget points of DWA. The USV will arrive at each subtarget point in turn and switch to the next target point within a certain range close to the subtarget point until it reaches the final target point. The motion is stopped after the target point, and the flow chart of the fusion algorithm is shown in Figure 9.

4. Improved DWA Simulation Experiment and Result Analysis

4.1. Improved DWA Simulation Results. The static obstacle avoidance simulation is carried out through the DWA of the original trajectory evaluation function and the improved trajectory evaluation function, respectively, and the obstacle avoidance effect of the DWA before and after the improvement is analyzed.

In the simulation experiment, the map size is set to 600 m × 400m, the position of the target point is set to (500, 50), the position of the starting point of the USV is (50, 350) and (50, 250), and the initial velocity and angular velocity of the USV are both 0. The DWA simulation of the original trajectory evaluation function is shown in Figure 10, and the DWA simulation under the improved trajectory evaluation function is shown in Figure 11.

It can be obtained from Figure 10 that when the USV faces a complex obstacle environment, the obstacle avoidance effect of the USV is not ideal. First, the USV is easy to fall into the concave area, and it takes a long time to escape the concave trap, which increases the length of the obstacle avoidance path. Second, when there is an obstacle near the target point, because the weight combination of the original trajectory evaluation function is relatively single, the distance evaluation function occupies a large weight value, which causes the target to be unreachable. USV stops moving when it is 20 meters away from the obstacle. The path planning effect is not ideal. As shown in Figure 11, the USV did not fall into the concave trap area but smoothly passed through the narrow channel and reached the target point smoothly. Compared with the original algorithm, the path length is reduced, and there is no target unreachable situation.

The path evaluation indicators before and after the improved DWA algorithm are shown in Table 4. It can be found that in the simulation environment of example (a), the improved DWA reduces the path length by 205.7 m compared with the original algorithm, accounting for 25.4% of the planned path length of the original algorithm. The smoothness is reduced by 0.98, accounting for 36.8% of the smoothness of the planned path of the original algorithm. The security degree is increased by 14, accounting for 14.14% of the security degree of the original algorithm. In the simulation environment of example (b), the path length of the improved DWA is reduced by 143 m compared with the original algorithm, accounting for 21.11% of the planned path length of the original algorithm. The smoothness is reduced by 0.84, accounting for 32.8% of the smoothness of the planned path of the original algorithm. The security is reduced by 5, accounting for 5.3% of the security of the planned path of the original algorithm. Because the original algorithm has the target unreachable situation, the security degree of its path evaluation index is lower than that of the improved DWA. In addition, the improved DWA integrates the fuzzy logic control algorithm, and the calculation amount is increased. In contrast, the path planning time is longer than the original algorithm, but the increase is not large.

To sum up, compared with the original DWA, the improved DWA shortens the planned path length by 23.4% and reduces the planned path smoothness by 34.8%. The introduction of the target distance to replace the direction angle

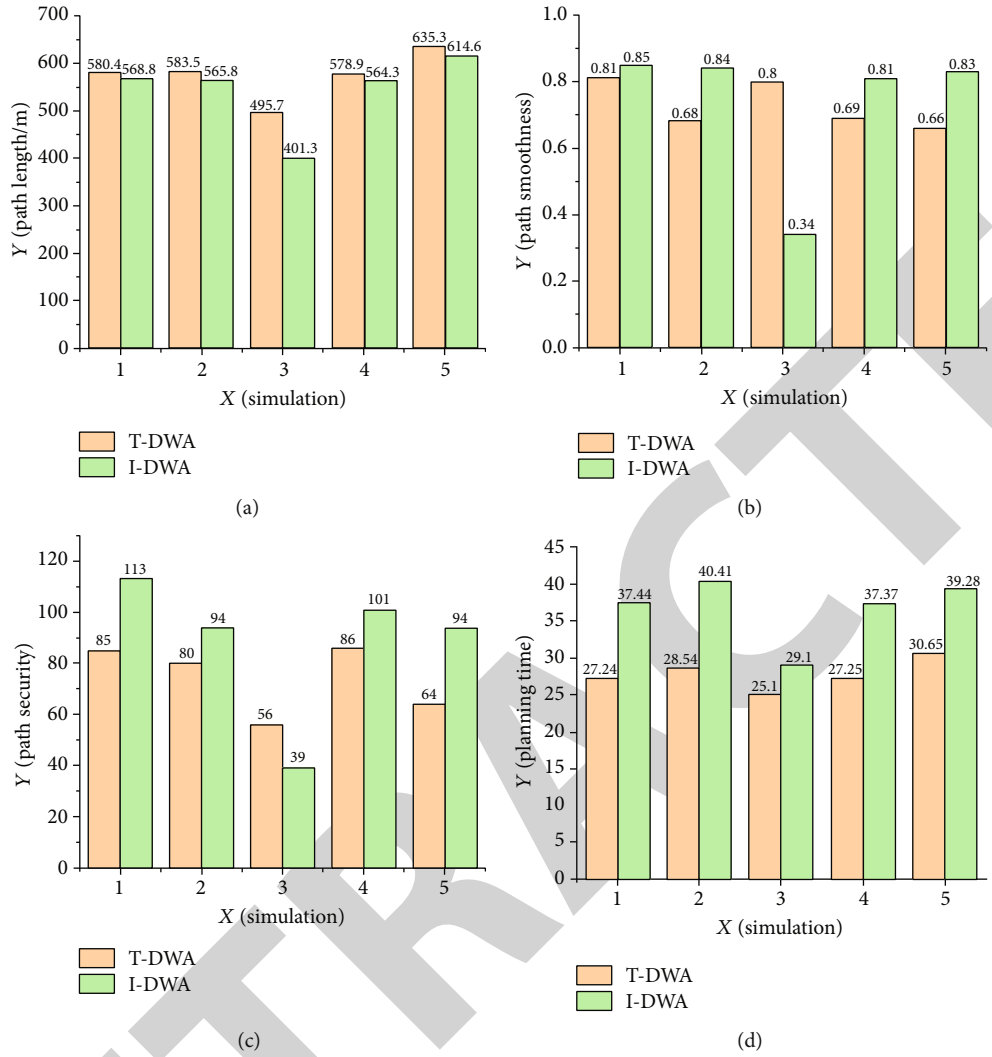

Figure 13: Performance comparison of traditional DWA and improved DWA.

difference and the fuzzy logic control algorithm to dynamically control the weight of the original trajectory evaluation function have a good improvement effect, which enhances the USV's adaptability to complex obstacle environments.

4.2. Simulation of Improved DWA with A∗ in Static Obstacle Environment. The A∗ algorithm is used to plan the known static obstacle environment and extract the subtarget points, while the local path planning algorithm performs local obstacle avoidance. In the simulation experiment, the map size is set to 600m × 400m, the target point position is set to (500, 50), and the USV starting point position is set to (50, 350). The simulation results of the fusion algorithm are shown in Figure 12.

By changing the position of the target point, to ensure that the parameters of each experiment are set to the same conditions, 5 simulation experiments are carried out for the algorithm before and after the improvement. The starting point is set to (50, 350), and the target points are set to (480, 50), (300, 50), (500, 100), and (550, 150).

Compare the traditional DWA and the improved DWA based on the A∗ algorithm, analyze the pros and cons of the planned paths before and after the algorithm improvement, and draw histograms according to the relevant data as shown in Figure 13.

Figure 13 shows the comparative effects of applying the traditional DWA method and the improved DWA method on various indicators, such as path length and path smoothness. Except for example 3, after improving DWA, the path length is reduced, but the path smoothness, security, and planning time are increased, indicating that the scheme of extracting subgoal points by the A∗ algorithm can shorten the length of the planned path and improve the operating efficiency of the USV, but it does not improve the smoothness and safety of the path. On the whole, compared with traditional DWA, the average path length is reduced by 5.53%, the average path smoothness is increased by 0.82%, the average path safety degree is increased by 18.87%, and the average planning time is increased by 32.3%.

The performance indicators of the improved DWA are not outstanding in all aspects, but in the complex obstacle environment, the USV cannot find the optimal path. The simulation results of example 3 show that compared with the

traditional DWA, the path length is reduced by 19.04%, and the smoothness is reduced by 57.5%, and the safety is reduced by 30.36%.

5. Conclusion

Through the analysis of the evaluation items of the DWA trajectory evaluation function and the weight setting of the evaluation function, it is found that the trajectory evaluation function has a great negative impact on the selection of the USV obstacle avoidance speed command when faced with a complex obstacle environment. Secondly, the derivative of the target distance is introduced to replace the evaluation item of the direction angle difference, and it improves the smoothness of the USV obstacle avoidance path. Finally, aiming at the solidification of the weights of each evaluation item of the trajectory evaluation function, the fuzzy logic control algorithm is integrated, and the obstacle distribution information obtained by the obstacle detection model is used as the controller input to dynamically adjust the weights. The effectiveness of the improved algorithm is verified by simulation.

Unmanned surface vehicles will develop in the direction of intelligence, and autonomous navigation and control technology is an important way for unmanned surface vehicles to achieve intelligence. This paper does not fully consider the path planning problem under the influence of dynamic obstacles in the marine environment. In addition, joint operations have become the basic combat style of marine warfare in the new era. As an emerging combat force, unmanned surface ships must be integrated into joint operations. Its accurate and efficient autonomous navigation technology is to explore the basis of other combat forces' coordinated operations, and it is necessary to conduct in-depth research on the path planning technology of unmanned surface vehicles.

Data Availability

The datasets generated during and/or analyzed during the current study are available from the corresponding author on reasonable request.

Conflicts of Interest

The authors declare that there is no conflict of interest regarding the publication of this paper.

Acknowledgments

This research is supported by the Fundamental Research Funds for the Central Universities (3072022JC040).

References

[1] B. Bovcon, J. Muhovi, D. Vranac, D. Mozeti, and M. Kristan, "MODS – a USV-oriented object detection and obstacle segmentation benchmark," *IEEE Transactions on Intelligent Transportation Systems*, vol. 23, no. 8, 2022.

[2] M. X. Zhou, R. Bachmayer, and B. DeYoung, "Surveying a floating iceberg with the USV SEADRAGON," *Frontiers in Marine Science*, vol. 8, p. 878, 2021.

[3] X. Liu, X. M. Ye, Q. B. Wang, W. Li, and H. Gao, "Review on the research of local path planning algorithms for unmanned surface vehicles," *Chinese Journal of Ship Research*, vol. 16, no. -Supp 1, pp. 1–10, 2021.

[4] C. Barrera, I. Padron, F. S. Luis, O. Llinas, and G. N. Marichal, "Trends and challenges in unmanned surface vehicles (USV): from survey to shipping," *Transnav-International Journal on Marine Navigation and Safety of Sea Transportation*, vol. 15, no. 1, pp. 135–142, 2021.

[5] J. F. Jimenez and J. M. Giron-Sierra, "USV based automatic deployment of booms along quayside mooring ships: scaled experiments and simulations," *Ocean Engineering*, vol. 207, 2020.

[6] T. T. Nguyen, N. H. Tran, T. M. D. Ho, and H. Nguyen, "Path planning for unmanned surface vehicle (USV) in obstacle-filled environments," in *2021 International Conference on Advanced Technologies for Communications (Atc 2021)*, pp. 104–108, Ho Chi Minh City, Vietnam, 2021.

[7] X. B. Liu, S. L. Zhou, Z. C. Xiao, Y. H. Qi, and F. Y. Dai, "Review on UAV obstacle avoidance methods," *Journal of Ordnance Equipment Engineering*, vol. 43, no. 5, pp. 40–47, 2022.

[8] Y. Yang, Z. Lin, M. Yue, G. Chen, and J. Sun, "Path planning of mobile robot with PSO-based APF and fuzzy-based DWA subject to moving obstacles," *Transactions of the Institute of Measurement and Control*, vol. 44, no. 1, pp. 121–132, 2022.

[9] K. Yan, W. Zheng, T. Zhang et al., "Cross-domain facial expression recognition based on transductive deep transfer learning," *IEEE Access*, vol. 7, pp. 108906–108915, 2019.

[10] M. Seder and I. Petrovic, "Dynamic window based approach to mobile robot motion control in the presence of moving obstacles," in *Proceedings of the 2007 Ieee International Conference on Robotics and Automation*, pp. 1986–1991, Rome, Italy, 2007.

[11] L. Chang, L. Shan, C. Jiang, and Y. Dai, "Reinforcement based mobile robot path planning with improved dynamic window approach in unknown environment," *Autonomous Robots*, vol. 45, no. 1, pp. 51–76, 2020.

[12] J. J. Liu, L. Q. Xue, H. J. Zhang, and Z. P. Liu, "Robot dynamic path planning integrating improved a∗ and DWA algorithm," *Computer Engineering and Application*, vol. 57, no. 15, pp. 73–81, 2021.

[13] L. Xu, W. H. Fu, and W. H. Jiang, "Mobile robot path planning based on 16 direction 24 neighborhood improved ant colony algorithm," *Control and Decision*, vol. 36, no. 5, pp. 1137–1146, 2021.

[14] X. Bai, H. Jiang, J. Cui, K. Lu, P. Chen, and M. Zhang, "UAV path planning based on improved A and DWA algorithms," *International Journal of Aerospace Engineering*, vol. 2021, Article ID 4511252, 12 pages, 2021.